Supporting Information

D-alanylation in the assembly of ansatrienin side chain is catalyzed by a modular NRPS

Guoyin Shi,[†,§] Ning Shi,[†,§] Yaoyao Li,[‡] Wang Chen,[‡] Jingjing Deng,[‡] Chao Liu,[†] Jing Zhu,[†] Haoxin Wang,[*,†] Yuemao Shen[*,†, ‡]

[†]State Key Laboratory of Microbial Technology, School of Life Sciences, Shandong University, Jinan, Shandong 250100, P. R. China

[‡]Key Laboratory of Chemical Biology (Ministry of Education), School of Pharmaceutical Sciences, Shandong University, Jinan, Shandong 250012, P. R. China

[§]These authors contributed equally to this work

*Correspondence to: wanghaoxin@sdu.edu.cn (H. Wang), yshen@sdu.edu.cn (Y. Shen).

Contents

1. General Methods

1.1. Strains, plasmids, and culture conditions

Bacterial strains and plasmids used in this study are listed in Table S1. The Streptomyces strains were cultured on SFM solid medium (1.5% agar, 2% D-mannitol, 2% soybean meal, pH 7.2 – 7.4) for conjugation, in YMG broth (0.4% yeast extract, 1% malt extract, 0.4% glucose, pH 7.2 – 7.4) for mycelial growth, and on YMG solid medium for fermentation.

Table S1. Bacteria strains and plasmids used in this study.

Strains or plasmids	Description	Reference or source
E.coli		
XL1-Blue	Host strain for general clone	Stratagene
EPI300	Host strain of fosmid vector	Epicentre
ET12567/pUZ8002	Host strain for conjugation between *E.coli* and *Streptomyces*	[1]
BW25113/pKD46	Host strain for PCR-targeting	[2]
BL21(DE3)	Host strain for protein expression	Novagen
Plasmids		
pJTU824	*Bla*, *tsr*, rep^{puc}, att^{C31}, *oriT*, *ermEP**	[3]
pJTU968	*bla*, *Perm*E*, pRSETb	
pPM927	pSAM2, *tsr*, *oriT*	[4]
pET28a(+)	Km^R, T7 Promoter, His6 Tag	Novagen
pET22b(+)	Amp^R, T7 Promoter, *pelB*, His6 Tag	Novagen

1.2. Fermentation and analysis of metabolites in the mutant strains

XZQH13 and its mutants were inoculated on YMG solid medium at 30 ℃ for 12 days. The culture was diced and extracted with AcOEt/MeOH/AcOH 80 : 15 : 5 (v/v/v) at room temperature. The extract was dissolved in MeOH and analyzed by HPLC (Agilent 1200 instrument; ZORBAX Eclipse XDB-C18 4.6 x 250 mm, 5 μm). HPLC chromatographic conditions were as follows. Water-0.035% TFA (solvent A) and acetonitrile-0.035% TFA (solvent B), flow rate: 1 mL min^{-1}; gradient: 5 to 35% B (5 min), increased to 55% B at 19 min, to 65% B at 20 min, to 100% B at 23 min, and back to 5% B from 28 min to 30 min. UV detection at 275 nm.

1.3. Fermentation, isolation and structure elucidation of compound 3

XZQH13Δ*astC* culture (17 liters) was allowed to grow on the Fermentation Medium at 30 ℃ for 12 days. The whole solid cultures were diced and extracted three times with AcOEt/MeOH/AcOH (80 : 15 : 5, v/v/v) at room temperature, and the crude extract solution was concentrated under reduced pressure, and the concentrated extract was sequentially solvent partitioned into petroleum ether-soluble extract and MeOH-

soluble extract. The MeOH extract was loaded to a Sephadex LH-20 column for separation. The column was eluted with MeOH to obtain seven fractions, Fr.1 - 7. Fr.5 (95 mg) was subjected to medium-pressure liquid chromatography (MPLC; 30 g RP-18 silica gel; MeOH/H_2O 30%, 40%, 50%, 70%, and 100%, 200 ml each) to afford six subfractions, Fr.5a – 5f. Fr.5e (15 mg) was subjected to preparative HPLC (Agilent 1200, ZORBAX Eclipse XDB-C18, 9.4×250 mm, 5 μm), using an isocratic solvent of 35% acetonitrile-0.04% TFA, at flow rate of 4 ml/min, detected at UV 274 nm. This afforded compound **3** (4 mg). To analyze the structure of compound **3**, 1D- and 2D-NMR were performed on a Bruker DRX-600 spectrometer. HRMS was carried out on a LTQ-Obitrap Velos Pro mass spectrometer (Thermo Scientific).

1.4. Expression of *astC, astF1* and *astC*$_{S545A}$ and purification

The genes *astC* and *astF1* was amplified from fosmid 17-10F via PCR by using primers listed in Table S2. The amplified fragments were digested with NdeI/HindIII and ligated with the NdeI/HindIII digested pET-28a(+) and pET-22b(+) vectors to generate pET-28a/*astC* and pET-22b/*astF1*, respectively. The active site Ser_{545} of T domain of AstC was mutated to Ala_{545} to obtain the inactivated $AstC_{S545A}$ by QuikChange method based on pET28a(+)/*astC* (Figure S1). The resulting plasmids were confirmed by DNA sequencing and then transformed into *E.coli* BL21(DE3) for protein expression. Picked colonies were grown in LB medium at 37 ℃ and 220 rpm overnight, then diluted 1:10 with fresh LB medium and grown at 37 ℃ and 220 rpm until OD_{600} = 0.6, then induced with 0.1 mM IPTG and incubated at 16 ℃ and 180 rpm overnight. The induced *E. coli* cells (1 L) were centrifuged at 4000 g for 15 min and resuspended in 15 ml lysis buffer (10 mM Tris-HCl pH8.0, 100 mM NaCl), and ultrasonicated on ice for 10 min at 3s on, 6s off intervals. After centrifugation for 30 min at 4 ℃ and 10000 *g*, the supernatant was applied onto Ni-NTA column (GE Healthcare, Ni Sepharose^{TM} 6 Fast Flow). The His_6-tagged AstC, $AstC_{S545A}$ and AstF1 proteins were both eluted with an elution buffer (10 mM Tris-HCl pH8.0, 100 mM NaCl, and 150 mM imidazole). Eluted fractions were analyzed by SDS-PAGE (Figure S2). Purified proteins were desalted on an Amicon ultra centrifugal filter unit (Ultracel-10K, 10,000 MWCO) with storage buffer (10 mM Tris-HCl pH8.0, 100 mM NaCl), and stored at -80 ℃ or in vitro assays.

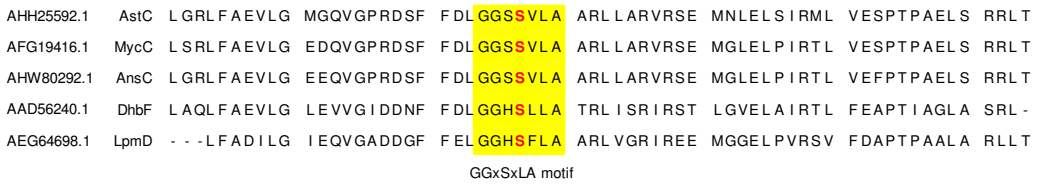

Figure S1. Alignment of the T domains of AstC and its analogs, MycC from *Streptomyces flaveolus*, AnsC from *Streptomyces seoulensis*, DhbF from *Bacillus subtilis* and LpmD from *Streptomyces viridochromogenes*.

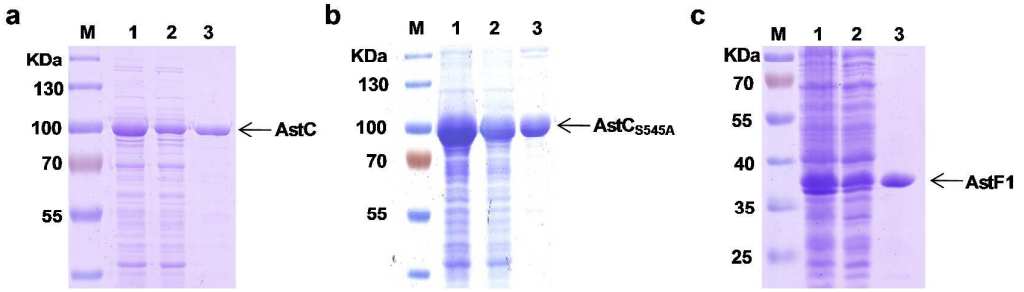

Figure S2. The SDS-PAGE of protein AstC (a), AstC$_{S545A}$ (b) and AstF1 (c). Lane M, molecular weight markers; Lane 1, crude cell extract after induced by 0.1 mM IPTG; Lane 2, supernatant of crude cell extract; Lane 3, protein eluted from Ni-NTA column.

1.5. HPLC chromatographic conditions

***In vitro* assays for AstC and AstC$_{S545A}$**: The supernatant was analyzed by HPLC (Thermo Finnigan Surveyor with an YMC Pack-Pro C18, 250 x 4.6 mm, 5 μm). Chromatographic conditions: solvent A: water with formic acid (0.1%); solvent B: acetonitrile with formic acid (0.1%); gradient: 20% B at 0–3 min, 45% B at 5–12 min, 100% B at 15–17 min, 20% B at 19–25 min; flow rate: 1 mL min^{-1}; UV detection at 260 nm. The electrospray ionization mass spectrometry (ESIMS) was carried out on a LTQ VELOS PRO ORBITRAP (Thermo, R = 30,000) in negative mode, equipped with an YMC Pack-Pro C18 column (250 x 4.6 mm, 5 μm) under the above HPLC conditions.

***In vitro* assay for AstF1:** Chromatographic conditions: solvent A: water with formic acid (0.1%); solvent B: acetonitrile with formic acid (0.1%); gradient: 20% B at 0–3 min, 45% B at 5–12 min, 63% B at 13 min, 90% B at 15–18 min, 100% B at 20–23 min, and 20% B at 24–30 min; flow rate: 1 mL min^{-1}; UV detection at 275 nm.

1.6. In vitro characterization of AstC

To determine the optimum pH, the reaction system A containing PBS (50 mM, pH 7.5), AstC (5 μM), Sfp (1 μM), CoA (100 μM), $MgCl_2$ (10 mM) and DTT (1 mM) was incubated for 1 h at 30 ℃. Then a 2 μL portion of reaction system A was mixed with 48 μL of reaction system B, which contains PBS (100 mM, pH range 6.0, 7.0, 8.0, 9.0, 10.0), compound **3** (26 μM), D-alanine (1 mM), ATP (2 mM), $MgCl_2$ (10 mM) and DTT (1 mM). After incubated at 30 ℃ for 30 min, 50 μL of methanol was added to quench the reaction. The optimal temperature for AstC activity was examined by incubating the mixture at pH 8.0 for 30 min at 20, 25, 30, 35, or 40 ℃, respectively. To detect the production of compound **4**, reactions with compound **3** (226 μM) were quenched at 0, 10, 20, 30, 45, 60, 180, or 300 min, respectively. Determination of the kinetic parameters of AstC was performed in a reaction volume of 20 μL containing varying concentrations of compound **3** at 1.66, 3.32, 6.65, 13.3, 26.6, 39.9, 53.2, 66.5, and 93.1 μM and fixed concentration of D-alanine at 0.2 mM, and D-alanine at 1, 2.5, 5, 8, 10, and 12 μM and fixed concentration of compound **3** at 33.25 μM, respectively. For the determination of reaction mechanism of AstC, reactions were performed with varying concentrations of D-alanine at 2.5, 5, 10, 15 or 20 μM with different constant concentrations of compound **3** at 0.67, 2.54, and 3.96 μM, respectively. All reactions were carried out in triplicate, and analyzed by HPLC as in vitro activity assay. Compound **4** was quantified using the peak areas based on the standard curve derived from analysis of different concentrations of compound **3**. The software GraphPad Prism 5 was used for the calculation of K_m and V_{max}. To determine substrate specificity of AstC, sodium propionate, β-alanine, D-Trp, D-Val, D-Phe, D-Tyr, D-Glu, D-Asp, D-Met, D-Arg, D-Ser, D-Pro, D-Thr, and Gly were tested as substrates, and the reactions were performed at optimized conditions for overnight, and analyzed by LC-MS as in vitro activity assay but in positive mode.

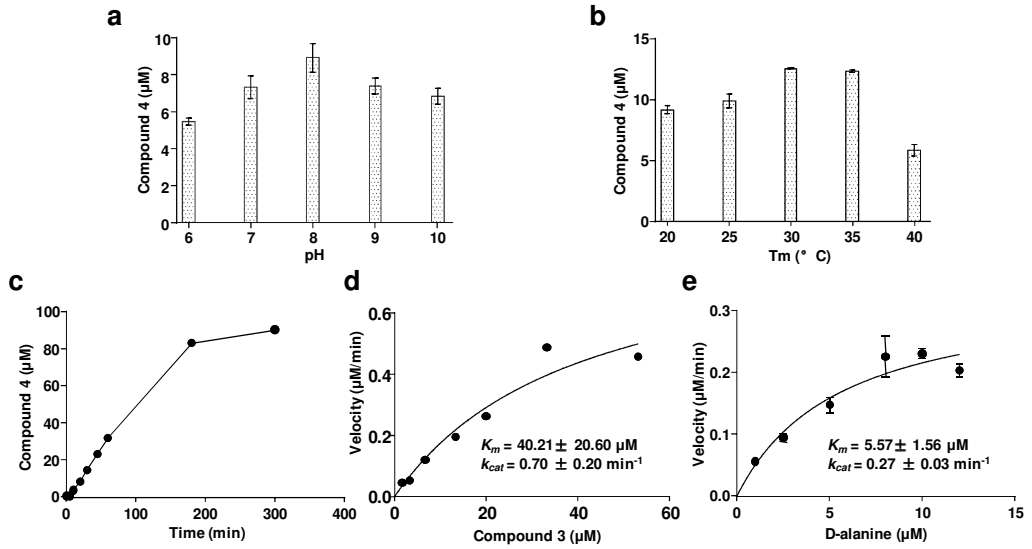

Figure S3. Characterization of AstC. a) pH optimum for **4** production catalyzed by AstC. b) Temperature optimum for **4** production catalyzed by AstC. c) The linear reaction phase of AstC. d) Kinetic characterization of AstC with varied concentration of **3**. e) Kinetic characterization of AstC with varied concentration of D-alanine.

1.7. Chemical synthesis of compounds I – VI

1.7.1. Chemistry

All chemicals, unless otherwise noted, were acquired from Sigma-Aldrich (St. Louis, MO) and were used as received without further purification. All water employed was ultrapure (> 18.2 MU cm^{-1} at 25 °C, Milli-Q, Millipore, Billerica, MA). All melting points were determined on a micro melting point apparatus and were uncorrected. ^{1}H NMR and ^{13}C NMR spectra were obtained on a Brucker Avance-400 NMR-spectrometer in the indicated solvents. Chemical shifts are expressed in ppm (d units) relative to TMS signal as internal reference. TLC was performed on Silica Gel GF254 and spots were visualized by iodine vapors or by irradiation with UV light (254 nm). Flash column chromatography was performed on column packed with Silica Gel 60 (200-300 mesh). Solvents were reagent grade and, when necessary, they were purified and dried by standard methods. Concentration of the reaction solutions involved the use of rotary evaporator at reduced pressure.

1.7.2. General procedure for the preparation of all *N*-acetylcysteamine (SNAc) thioester derivatives (Scheme 1)

Scheme 1. The synthesis of *N*-acetylcysteamine (SNAc) thioester derivatives

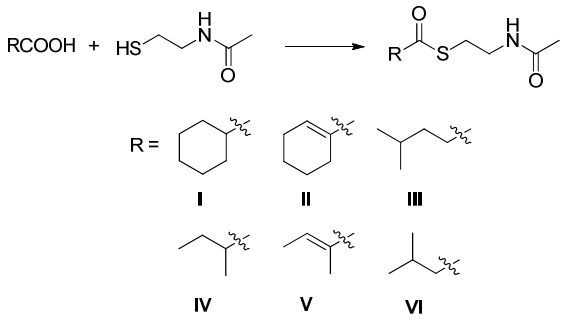

Reagents and conditions: DMAP, EDC·HCl, DCM, r.t. overnight.

To a solution of *N*-acetylcysteamine (120 mg, 1 mmol, 1 eq) in dichloromethane (10 mL) was added the appropriate acid (1.2 mmol, 1.2 eq), (3-dimethylaminopropyl)-3-ethylcarbodiimide hydrochloride (EDC·HCl, 2 mmol, 2 eq) and *N,N*-dimethylpyridin-4-amine (DMAP, cat.) under nitrogen. The reaction mixture was stirred overnight and treated with water and dichloromethane. The organic layer was washed with saturated $NaHCO_3$ solution and brine. The organic phases were combined and dried over and evaporated to dryness under reduced pressure. Purification by chromatography using petroleum ether/acetone 50:1–10:1 yielded corresponding compound.

1.7.3. Characterization data

S-(2-acetamidoethyl)-cyclohexanecarbothioate (**I**). Yield: 63%; colorless oil. ^{1}H-NMR (400 MHz, $CDCl_3$, r.t.) δ 6.09 (s, br, 1H), 3.42 (dd, J = 12.4, 6.2 Hz, 2H), 3.01 (t, J = 6.5 Hz, 2H), 2.51 (tt, J = 11.5, 3.5 Hz, 1H), 1.97 (s, 3H), 1.95 – 1.86 (m, 2H), 1.84 – 1.74 (m, 2H), 1.66 (dd, J = 7.7, 6.5 Hz, 1H), 1.45 (dq, J = 12.2, 2.9 Hz, 2H), 1.25 (ddq, J = 11.9, 8.9, 3.0 Hz, 3H); ^{13}C-NMR (101 MHz, $CDCl_3$, r.t.) δ 203.68, 170.38, 52.69, 39.77, 29.53, 28.00, 25.54, 25.42, 23.13. HR-ESI-MS: *m/z* 230.1206 $[M + H]^+$.

S-(2-acetamidoethyl)-cyclohex-1-enecarbothioate (**II**). Yield: 56%; colorless powder; mp: 68–70℃. ^{1}H-NMR (400 MHz, $CDCl_3$, r.t.) δ 7.08 – 6.94 (m, 1H), 5.97 (s, br, 1H), 3.45 (dd, J = 12.2, 6.0 Hz, 2H), 3.07 (t, J = 6.4 Hz, 2H), 2.38 – 2.26 (m, 2H), 2.26 – 2.19 (m, 2H), 1.97 (s, 3H), 1.75 – 1.55 (m, 4H); ^{13}C-NMR (101 MHz, $CDCl_3$, r.t.) δ 193.21, 170.27, 139.39, 138.27, 39.93, 28.05, 25.89, 24.07, 23.24, 21.90, 21.50. HR-ESI-MS: *m/z* 228.1047 $[M + H]^+$.

S-(2-acetamidoethyl)-4-methylpentanethioate (**III**). Yield: 61%; colorless oil. ^{1}H-NMR (400 MHz, $CDCl_3$, r.t.) δ 6.43 (s, br, 1H), 3.42 (q, J = 6.3 Hz, 2H), 3.02 (t, J =

6.6 Hz, 2H), 2.60 – 2.55 (m, 2H), 1.98 (s, 3H), 1.65 – 1.49 (m, 3H), 0.91 (s, 3H), 0.90 (s, 3H); ^{13}C-NMR (101 MHz, $CDCl_3$, r.t.) δ 200.15, 170.62, 42.19, 39.62, 34.32, 28.33, 27.54, 23.02, 22.16. HR-ESI-MS: *m/z* 218.1202 $[M + H]^+$.

S-(2-acetamidoethyl)-2-methylbutanethioate (**IV**). Yield: 52%; colorless oil. ^{1}H-NMR (400 MHz, $CDCl_3$, r.t.) δ 6.24 (s, br, 1H), 3.43 (dd, J = 12.4, 6.2 Hz, 2H), 3.03 (t, J = 6.5 Hz, 2H), 2.66 – 2.51 (m, 1H), 1.98 (s, 3H), 1.79 – 1.66 (m, 1H), 1.57 – 1.40 (m, 1H), 1.17 (d, J = 6.9 Hz, 3H), 0.92 (t, J = 7.4 Hz, 3H); ^{13}C-NMR (101 MHz, $CDCl_3$, r.t.) δ 204.40, 170.55, 50.16, 39.79, 28.05, 27.11, 23.06, 17.14, 11.52. HR-ESI-MS: *m/z* 204.1045 $[M + H]^+$.

(E)-S-(2-acetamidoethyl)-2-methylbut-2-enethioate (**V**). Yield: 71%; colorless oil. ^{1}H-NMR (400 MHz, $CDCl_3$, r.t.) δ 6.87 (dd, J = 6.9, 1.3 Hz, 1H), 6.01 (s, br, 1H), 3.45 (dd, J = 12.3, 6.1 Hz, 2H), 3.07 (t, J = 6.4 Hz, 2H), 1.97 (s, 3H), 1.88 (s, 3H), 1.85 (dd, J = 7.0, 0.9 Hz, 3H); ^{13}C-NMR (101 MHz, $CDCl_3$, r.t.) δ 193.85, 170.37, 136.86, 136.82, 39.89, 28.35, 23.20, 14.46, 12.14. HR-ESI-MS: *m/z* 202.0894 $[M + H]^+$.

S-(2-acetamidoethyl)-3-methylbutanethioate (**VI**). Yield: 42%; colorless oil. ^{1}H-NMR (400 MHz, $CDCl_3$, r.t.) δ 6.30 (s, br, 1H), 3.43 (dd, J = 12.4, 6.3 Hz, 2H), 3.03 (t, J = 6.5 Hz, 2H), 2.46 (d, J = 7.1 Hz, 2H), 2.24 – 2.07 (m, 1H), 1.98 (s, 3H), 0.97 (s, 3H), 0.95 (s, 3H); ^{13}C-NMR (101 MHz, $CDCl_3$, r.t.) δ 199.47, 170.48, 52.83, 39.71, 28.36, 26.45, 23.08, 22.19. HR-ESI-MS: *m/z* 204.1046 $[M + H]^+$.

Table S2. Primers used in this study.

Screening of library	
fosmid 17-10F	AHBAF: CCSGCCTTCACCTTCATCTCCTC AHBAR2: AYCCGGAACATSGCCATGTAGTG
Gene disruption	
astD1	AprQH13PKS-F: TGCCCGTCTGCTGTCGCCCCGGAAGGATGACGACACATGATTCCGGG GATCCGTCGACC AprQH13PKS-R: CGTCCCGTCGGGGTCGAGCAGCGGCCGCGGCGCCGCCTCTGTAGGC TGGAGCTGCTTC
astC	AprQH13*astC*-F: CCGTCTGACGGCACCCCGGCGAGAATTCGTACGAACCCTATTCCGGGG ATCCGTCGACC AprQH13*astC*-R: GATGCCCAGGTGGTAGGTGATGGCTGTCTCCCGGACCGCTGTAGGCT GGAGCTGCTTC
astF1	AprQH13*astF1*-F: GCCGCCACGCACACGACTGAGATCCGAGGACACGACACCATTCCGGG GATCCGTCGACC AprQH13*astF1*-R : GTCTCCACAGGGTTCGTACGAATTCTCGCCGGGGTGCCGTGTAGGCTG GAGCTGCTTC
Gene complementation	
astC	*astC*-C-F: GAGGCGGACATATGGAGACGAACATGCTGGTGCAG *astC*-C-R: TACGAATTCTCAGTCGGCGAGGTGGCCGGAGAC
astF1	*astF1*-C-F: GAGGCGGACATATGCCCCAGATACAGACGGCGGAA *astF1*-C-R: TACGAATTCTCAGACGGCCGGGGTGCGCATCCA
Vector	SBTF: GAGCGGATAACAATTTCACACAGG
Verification of gene disruption	
astD1	PKS-check-F: GAGGAGTTACGGGTGGCAAGA PKS-check-R: GCGAGGAGCACAGGACGAACG
astC	*astC*-check-F: CGTCGCACACCTGGTCTGCCAGGCCGTCAA *astC*-check-R: GCGCAGACGACGTCCGCGGCGGCGAAGGCA
astF1	*astF1*-check-F: ACACGACTGAGATCCGAGGACACG *astF1*-check-F: CAGCATGTTCGTCTCCACAGGGTT
Protein expression	
AstC	AstC-F-Nde I : GGAATTCCAT ATGGAGACGAACATGCTGGTGCAGG AstC-R-HindIII: CCCAAGCTT TCAGTCGGCGAGGTGGCCGGAGACG
AstF1	AstF1-F-Nde I: GGAATTCCAT ATGCCCCAGATACAGACGGCGGAAG AstF1-R-Hind III : CCCAAGCTT GACGGCCGGGGTGCGCATCCAG
Site-directed mutagenesis	
$astC_{S545A}$	AstC-S545A-F: GACCTCGGCGGCTCCG**C**CGTGCTGGCGGCCCGG AstC-S545A-R: CCGGGCCGCCAGCACG**G**CGGAGCCGCCGAGGTC

Table S3. The ^{1}H- and ^{13}C-NMR spectroscopic data for **3** (DMSO-d_6). At 600 and 150 MHz, respectively; *J* in ppm.

Position	δ_H	δ_C	Position	δ_H	δ_C
1		170.4s	15	4.94 (d, 7.5)	122.5d
2	2.82 (dd, 12.7, 4.3)	41.9t	16	2.17 (m)	25.9t
	2.61 (m)			1.95 (m)	
3	4.07 (m)	79.5d	17	2.76 (m)	28.5t
				2.62 (m)	
4	5.45 (dd, 15.2, 8.5)	129.9d	18		128.3s
5	6.17 (m)[a]	134.7d	19		143.1s
6	6.06 (m)	128.1d	20		124.7s
7	6.17 (m)[a]	134.5d	21	6.86 (d, 6.9)	109.6d
8	6.02 (m)	131.6d	22		129.9s
9	5.81 (m)	132.5d	22a		165.1s
10	2.33 (m)	36.1t	23		
	2.16 (m)				
11	3.48 (m)	70.1d	23a	3.39 (d, 14.8)	29.1t
				3.33 (d, 14.8)	
12	1.47 (m)	40.4d	12a	0.67 (d, 6.7)	10.0q
13	4.61 (br s)	67.2d	14a	1.63 (s)	21.1q
14		140.2s	MeO-3	3.22 (s)	55.7q

[a]Signals overlapped.

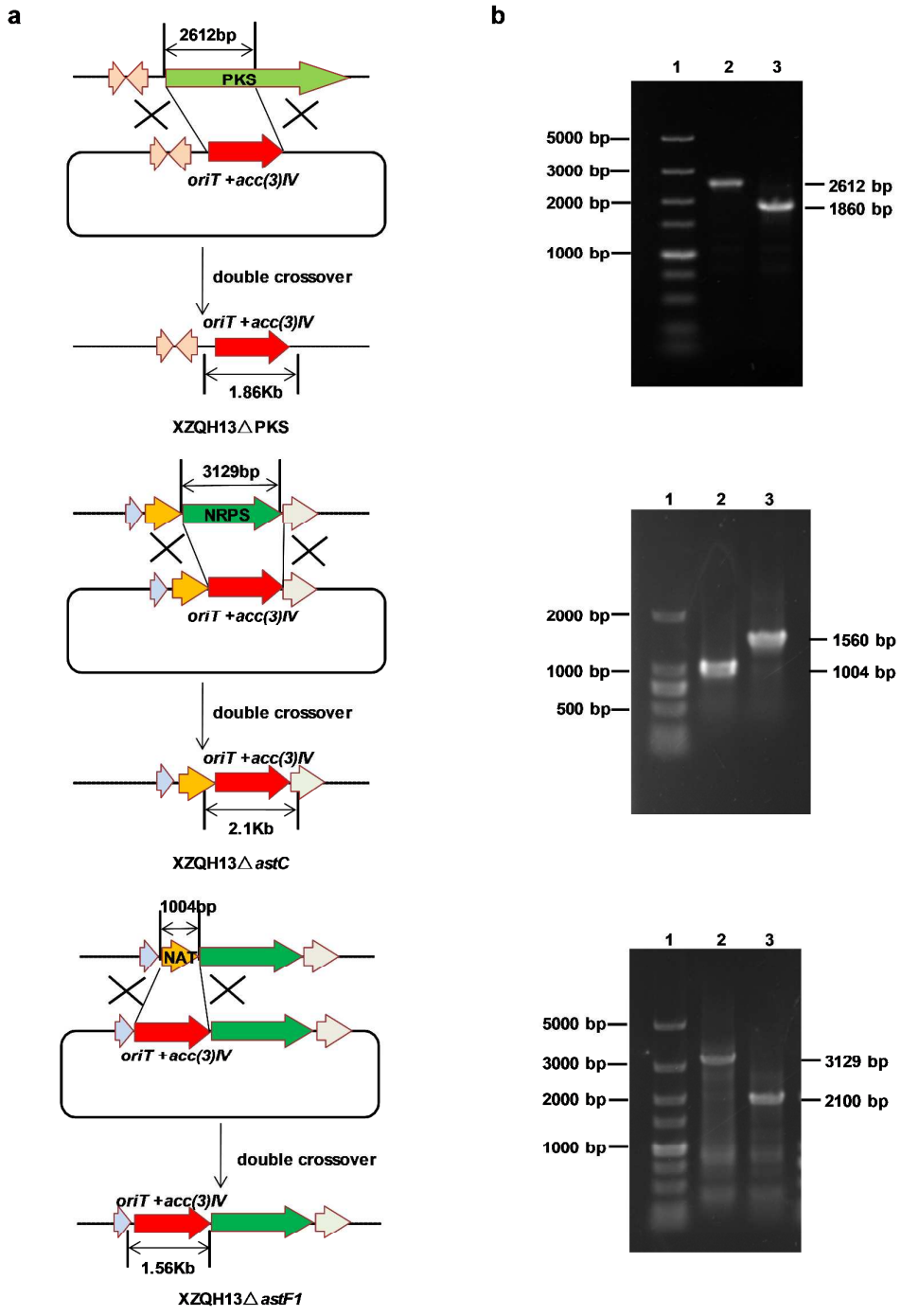

Figure S4. Disruption of the *astD1*, *astC* and *astF1* genes. a) Schemes of the gene inactivation of *astD1*, *astC* and *astF1*. *aac(3)IV*: apramycin resistance gene. b) PCR amplification using check primers confirmed the genotype of double crossover mutants. Lane 1, DNA ladder; lane 2, PCR product of the strain XZQH13/pJTU824-*astG1* (OE); lane 3, PCR products of the mutant strains XZQH13OEΔ*astD1* (top), XZQH13OEΔ*astC* (middle) and XZQH13OEΔ*astF1* (bottom).

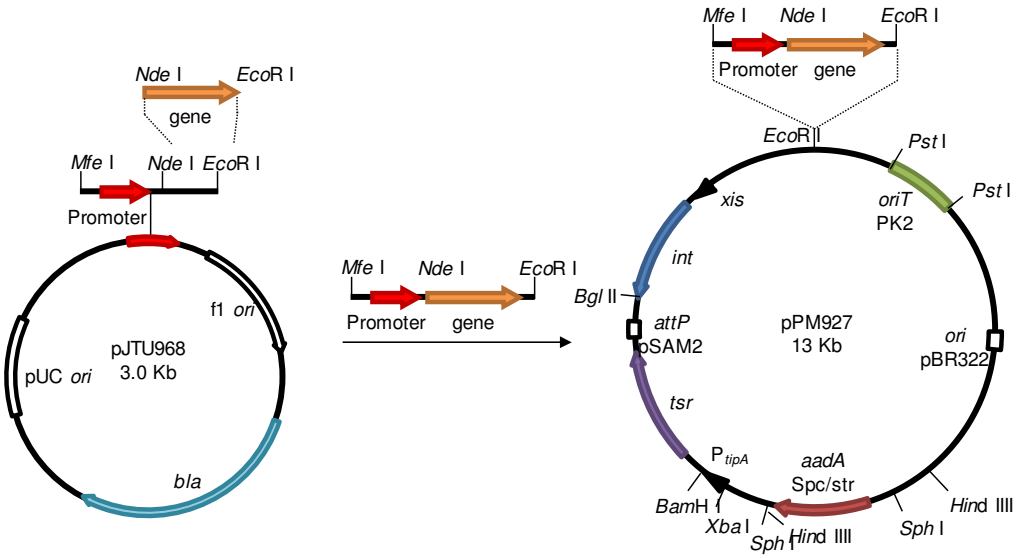

Figure S5. Complementation for the *astC* and *astF1* genes. The *astF1* and *astC* genes were amplified from plasmid 17-10F using the primers listed in Table S2. The PCR products were first purified, cloned into the pJTU968 vector, and sequenced to verify the inserted DNA sequence, then digested and ligated into pPM927, generating the complementation plasmids pPM927-*astF1* and pPM927-*astC*, respectively. The two plasmids were introduced into the mutant strains XZQH13OEΔ*astC* and XZQH13OEΔ*astF1* by conjugation, respectively. Spectinomycin-resistant exconjugants were selected and verified by PCR amplifications with the primers listed in Table S2 to confirm that the desired mutants had been generated. *aadA*: spectinomycin resistance gene.

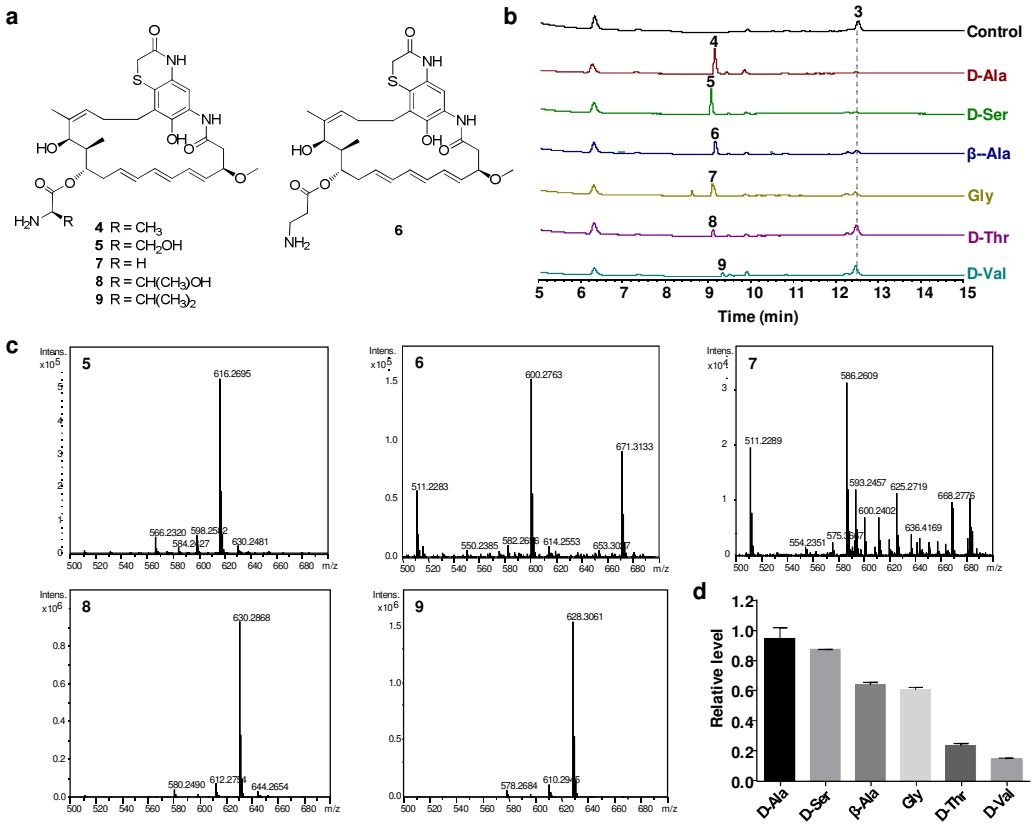

Figure S6. Substrate specificity of AstC. a) The chemical structures of **4** – **9**. b) HPLC traces (260 nm) showing products resulting from incubation of various amino acids and **3** with *holo*-AstC. The reaction with boiled AstC served as control. c) The mass spectrum of compounds **5** – **9**. d) The relative turnover ratios were determined by measuring the peak areas of the corresponding products referenced to the peak (**4**) detected in the D-alanine-containing assay.

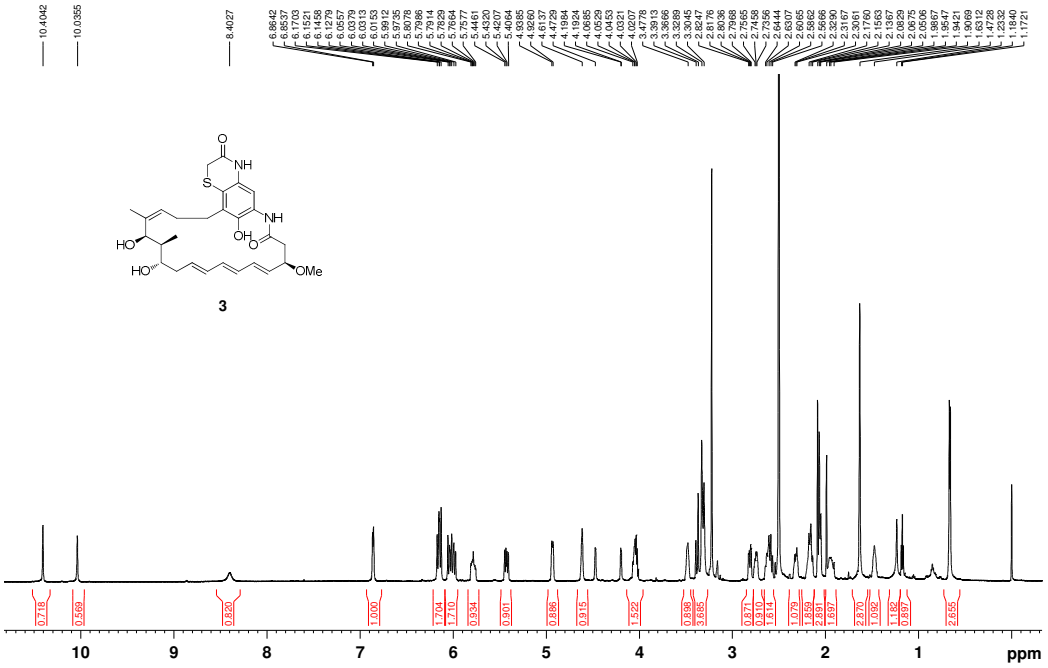

Figure S7. The ^{1}H-NMR spectrum of **3** in DMSO-d_6.

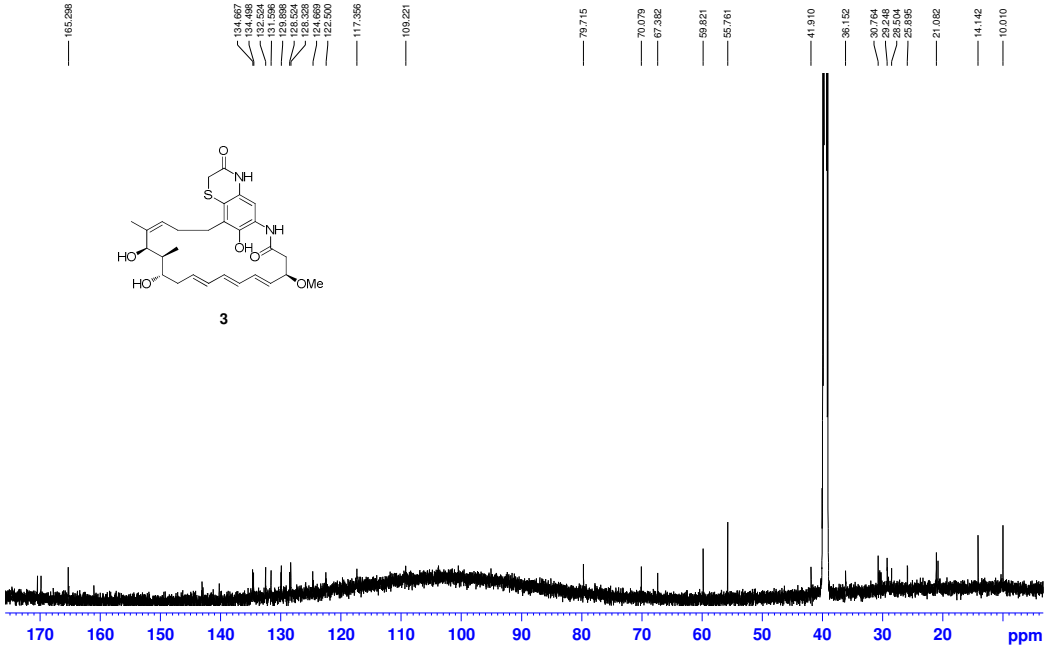

Figure S8. The ^{13}C-NMR spectrum of **3** in DMSO-d_6.

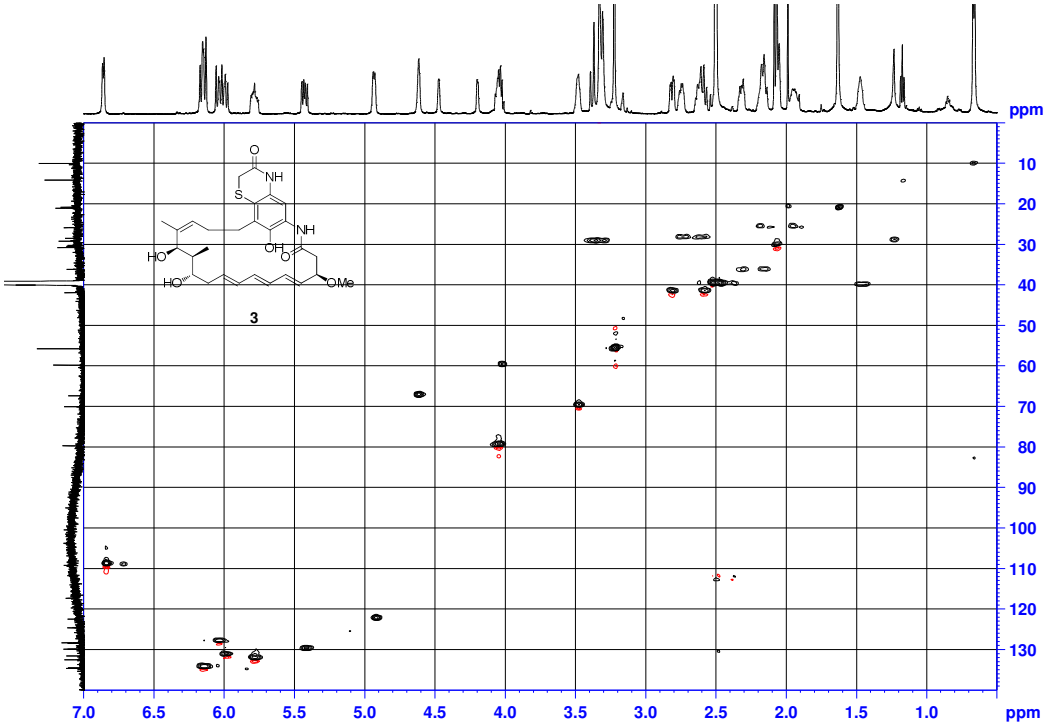

Figure S9. The HSQC spectrum of **3** in DMSO-d_6.

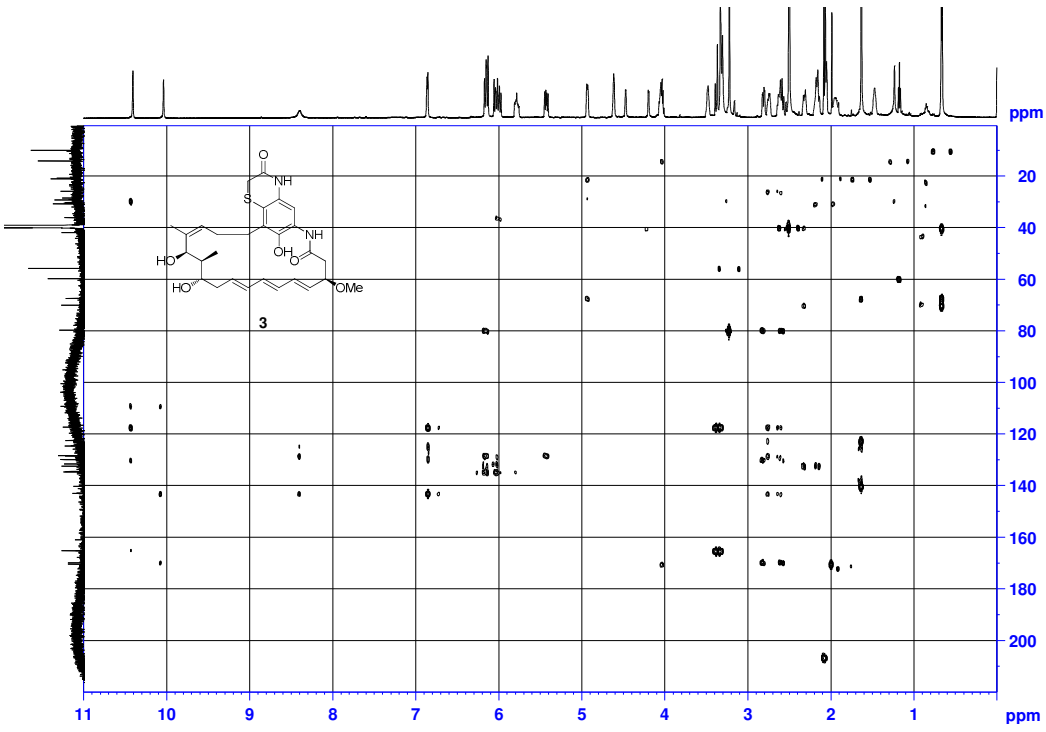

Figure S10. The HMBC spectrum of **3** in DMSO-d_6.

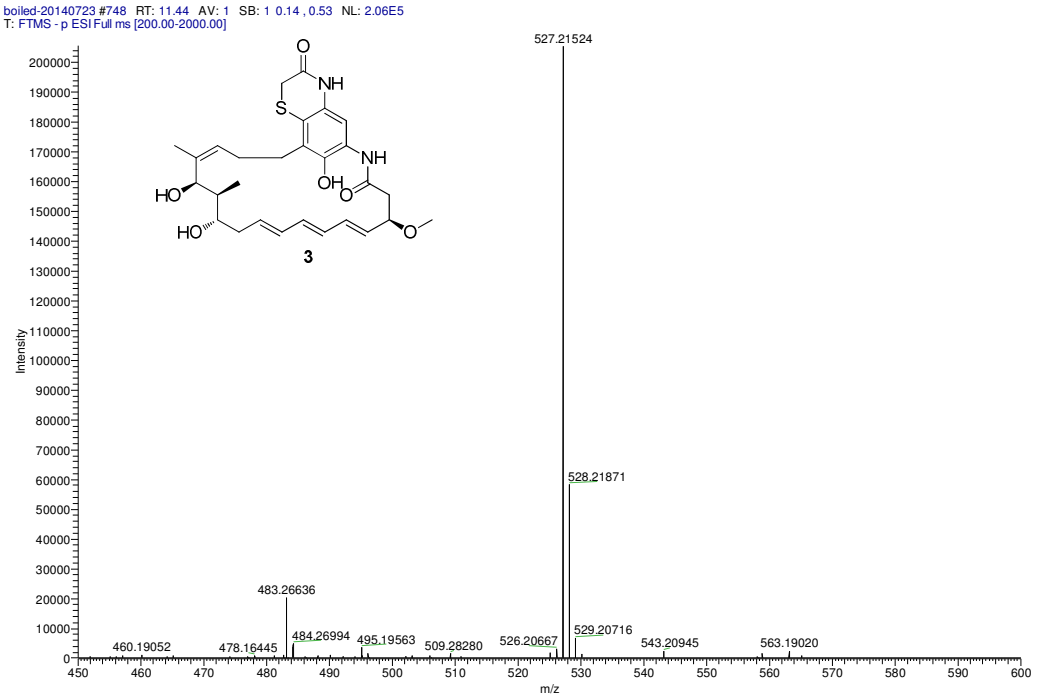

Figure S11. The HRESI mass spectrum of **3**.

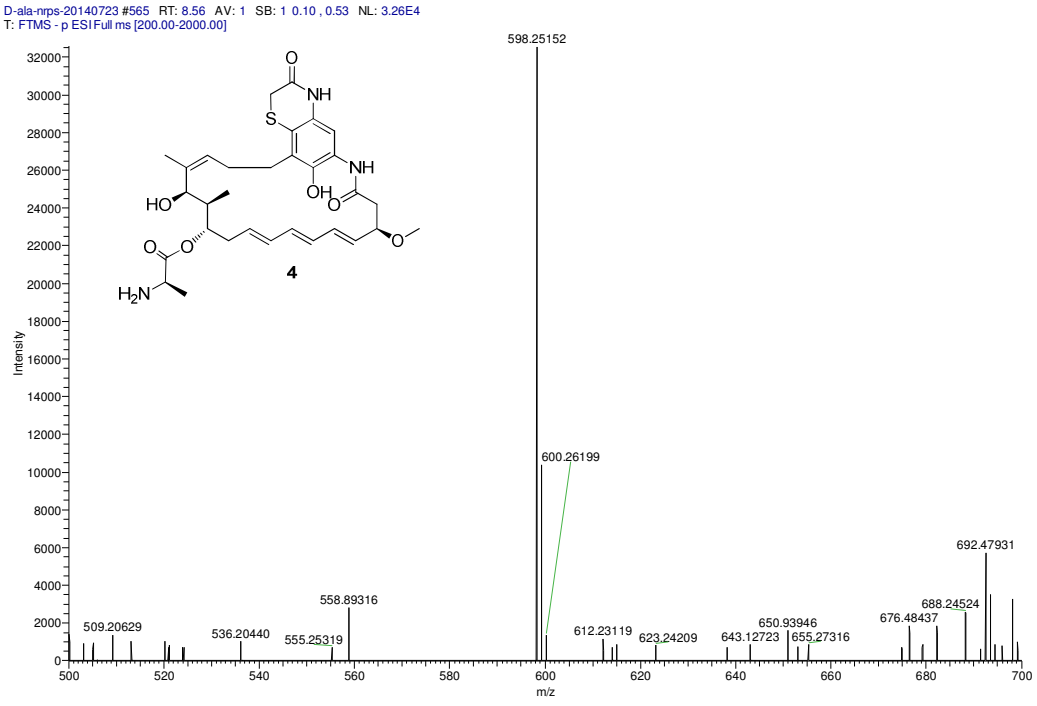

Figure S12. The HRESI mass spectrum of **4**.

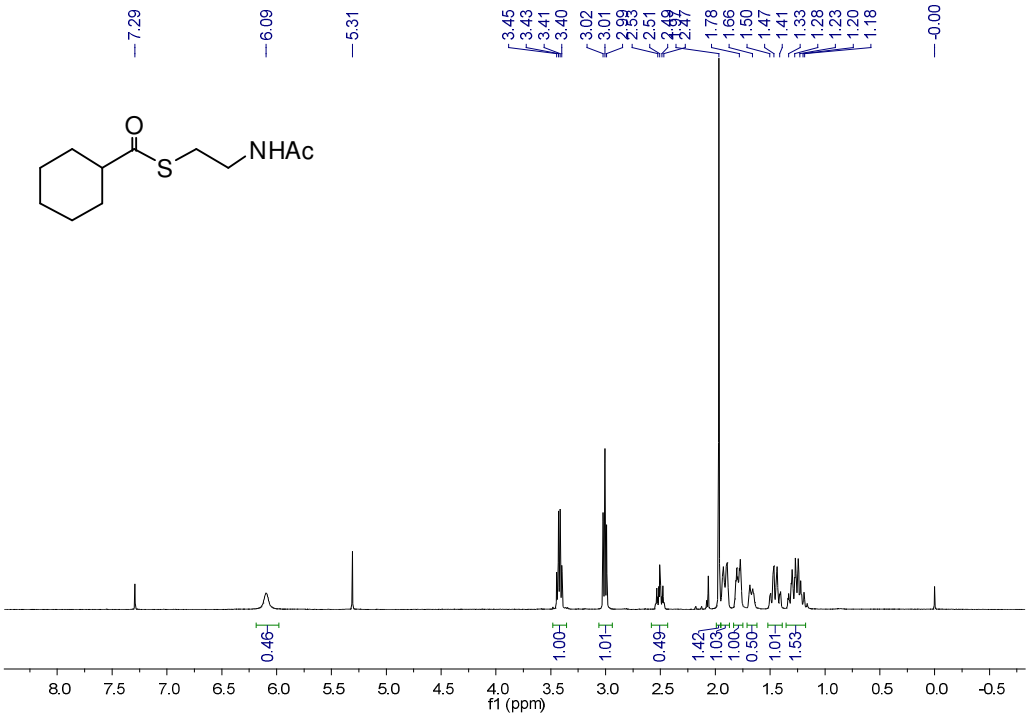

Figure S13. The ^{1}H-NMR (400 MHz, $CDCl_3$, r.t.) spectrum of **I**.

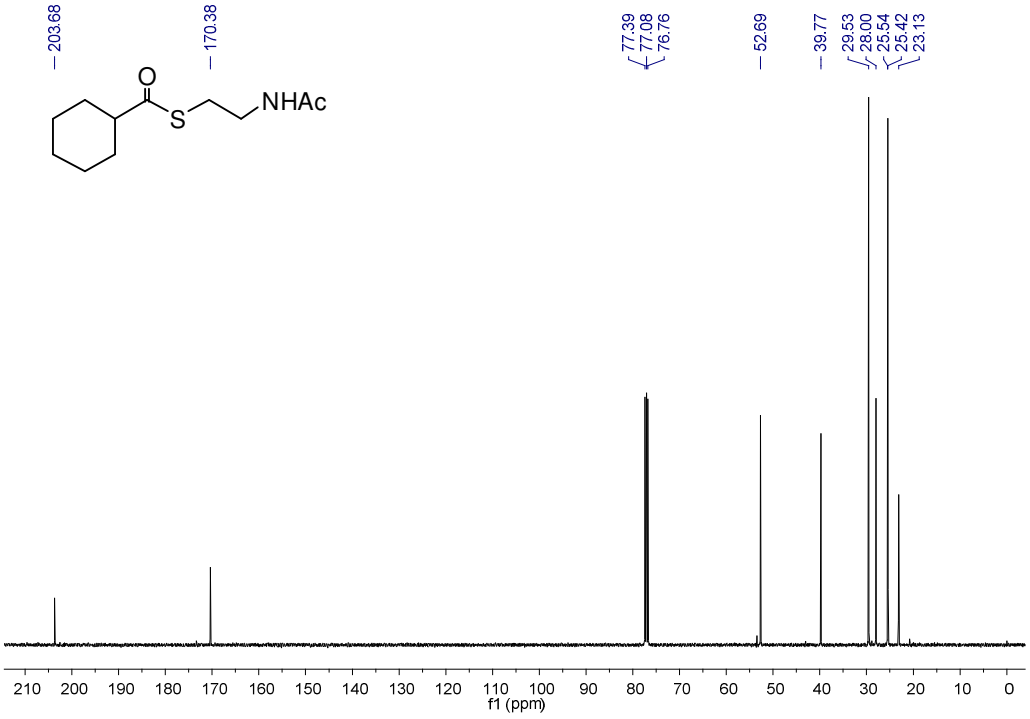

Figure S14. The ^{13}C-NMR (100 MHz, $CDCl_3$, r.t.) spectrum of **I**.

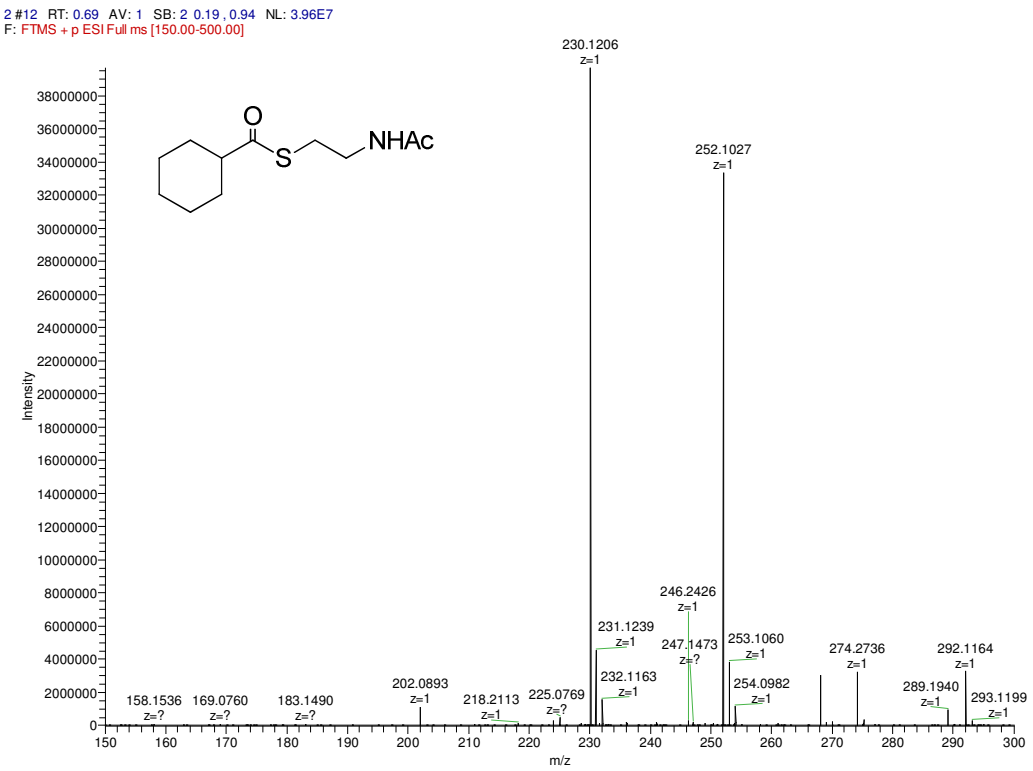

Figure S15. The HRESI mass spectrum of **I**.

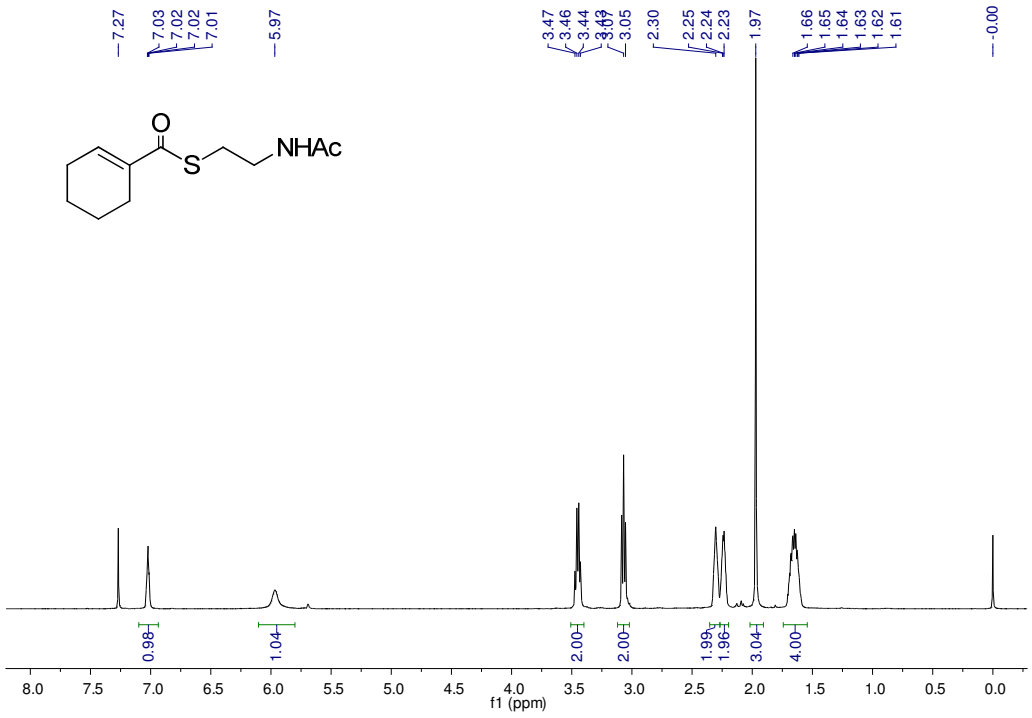

Figure S16. The ^{1}H-NMR (400 MHz, $CDCl_3$, r.t.) spectrum of **II**.

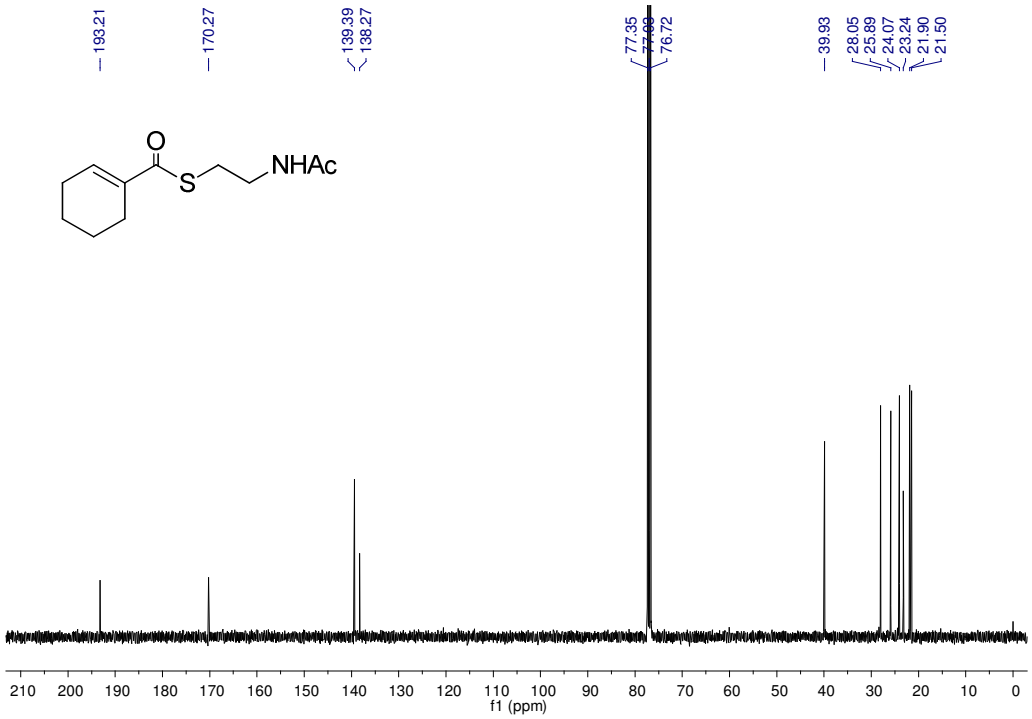

Figure S17. The ^{13}C-NMR (100 MHz, $CDCl_3$, r.t.) spectrum of **II**.

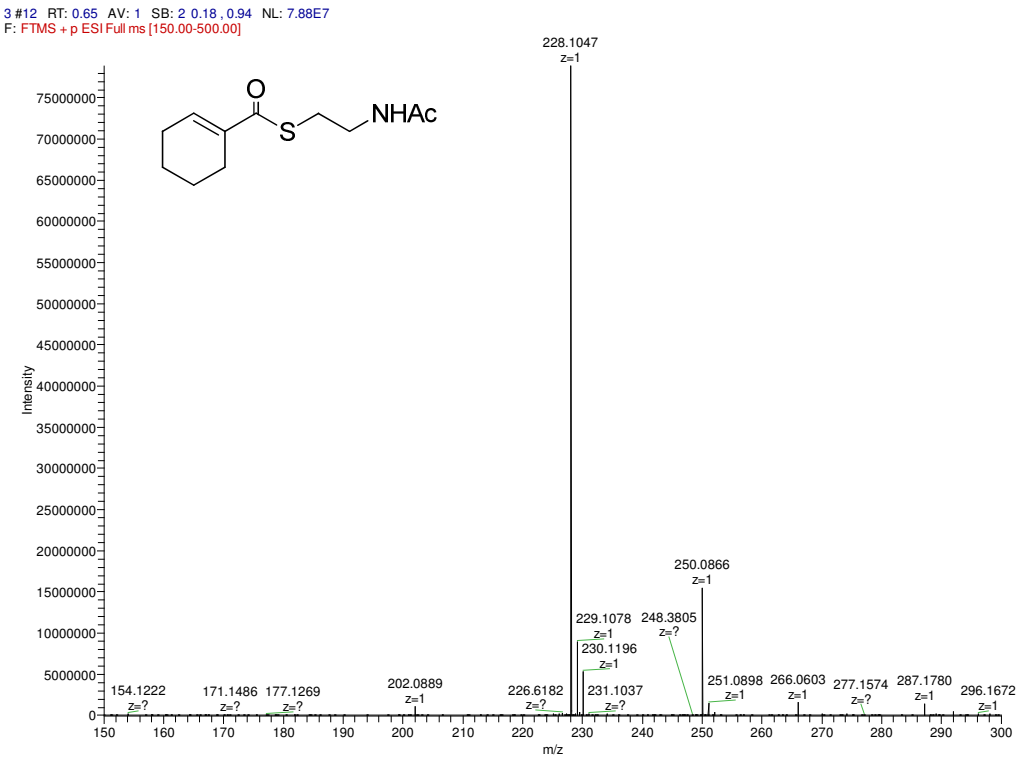

Figure S18. The HRESI mass spectrum of **II**.

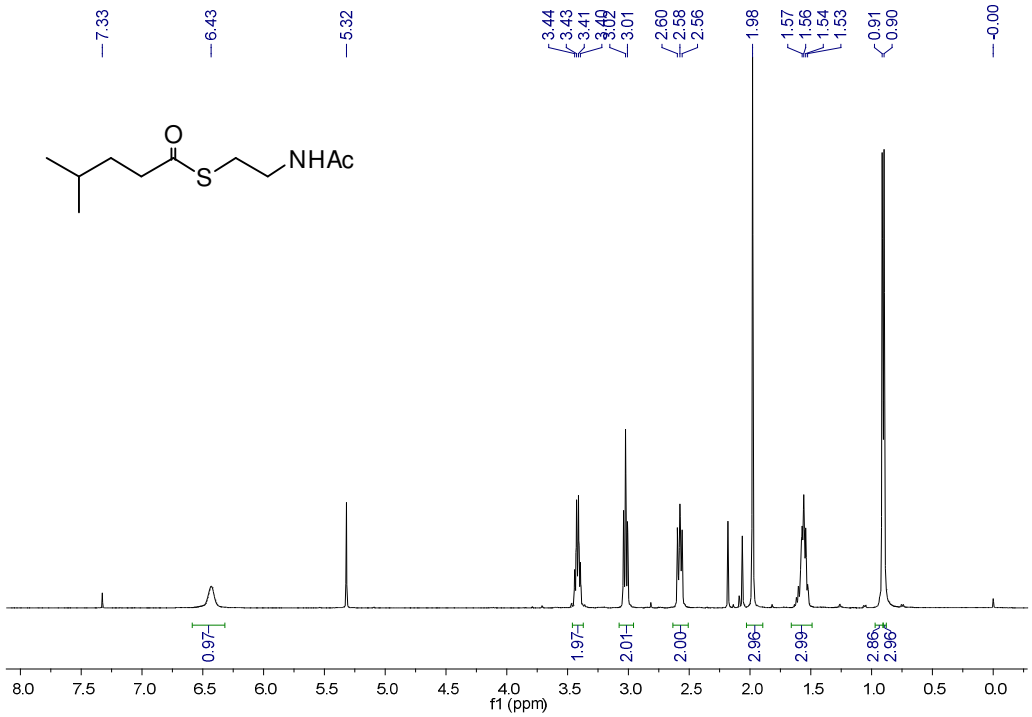

Figure S19. The ^{1}H-NMR (400 MHz, $CDCl_3$, r.t.) spectrum of **III**.

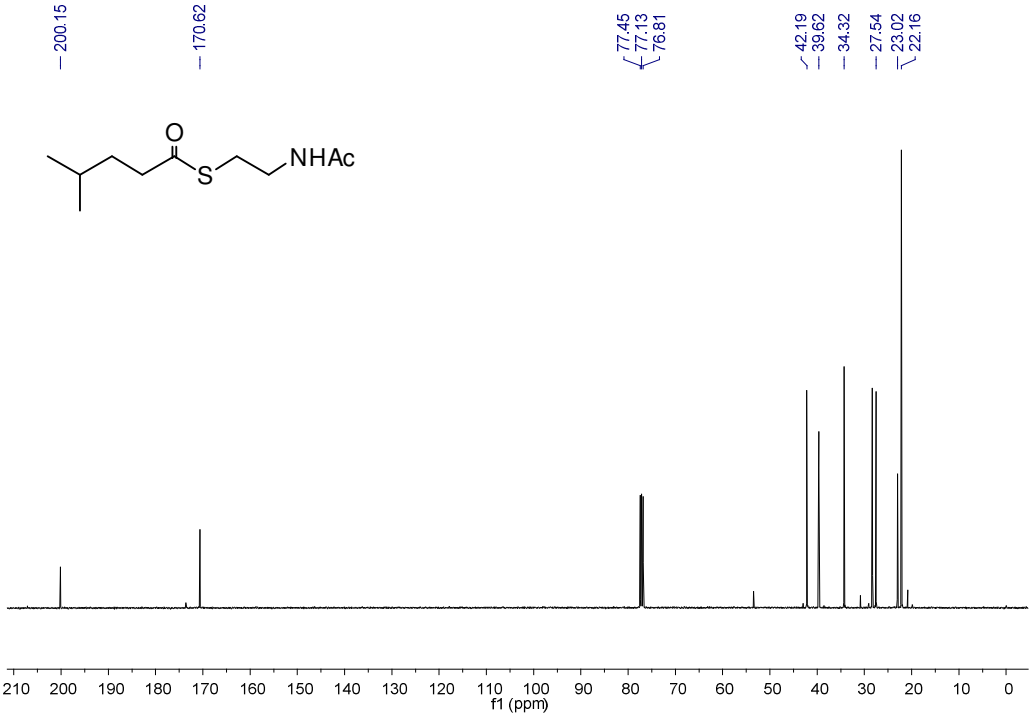

Figure S20. The ^{13}C-NMR (100 MHz, $CDCl_3$, r.t.) spectrum of **III**.

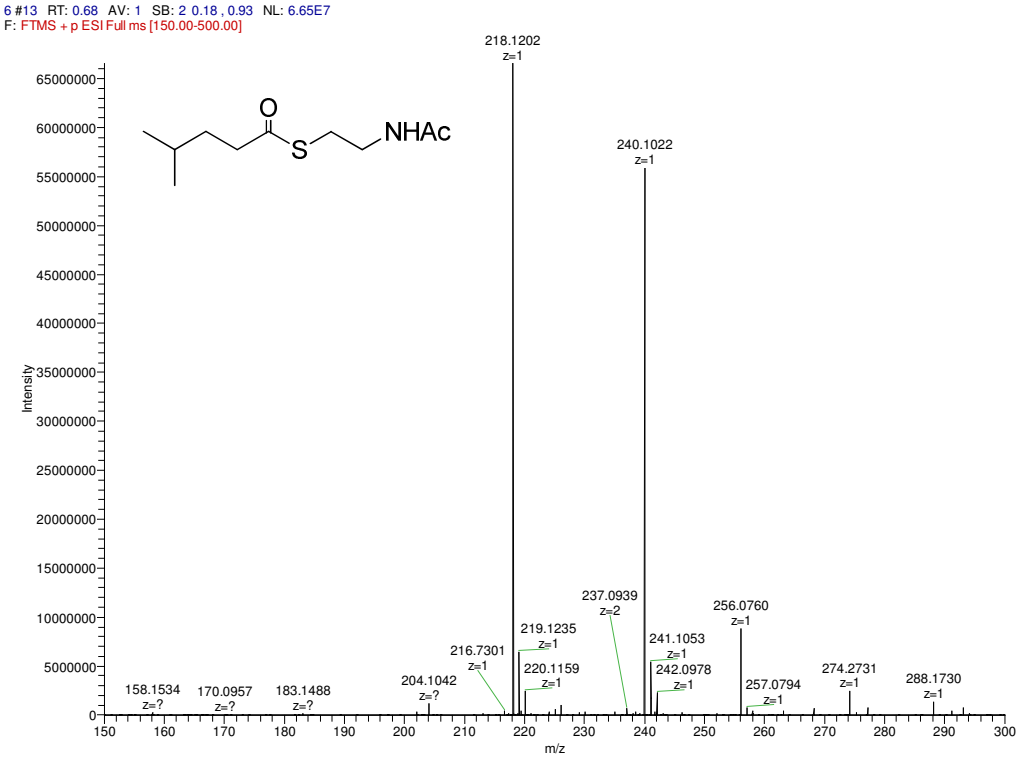

Figure S21. The HRESI mass spectrum of **III**.

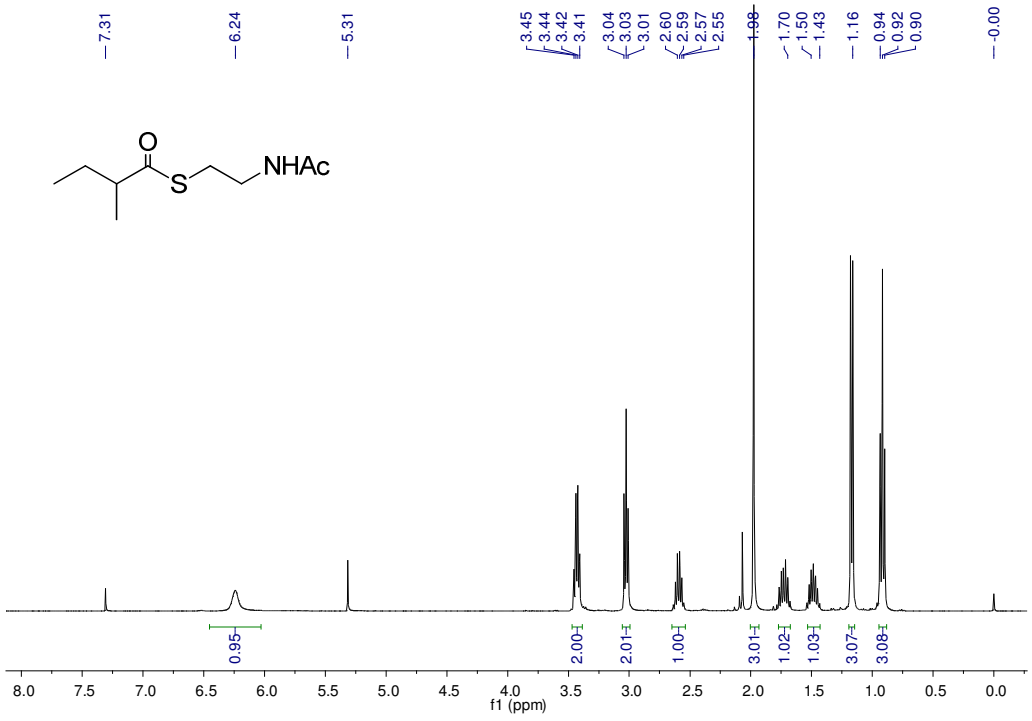

Figure S22. The ^{1}H-NMR (400 MHz, $CDCl_3$, r.t.) spectrum of **IV**.

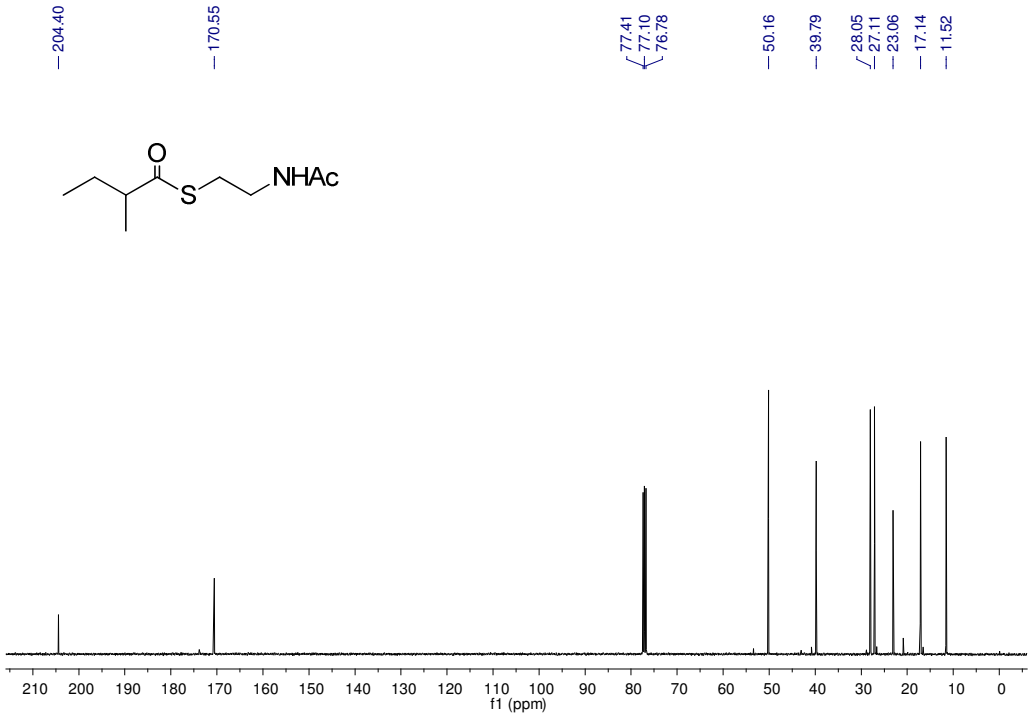

Figure S23. The ^{13}C-NMR (100 MHz, $CDCl_3$, r.t.) spectrum of **IV**.

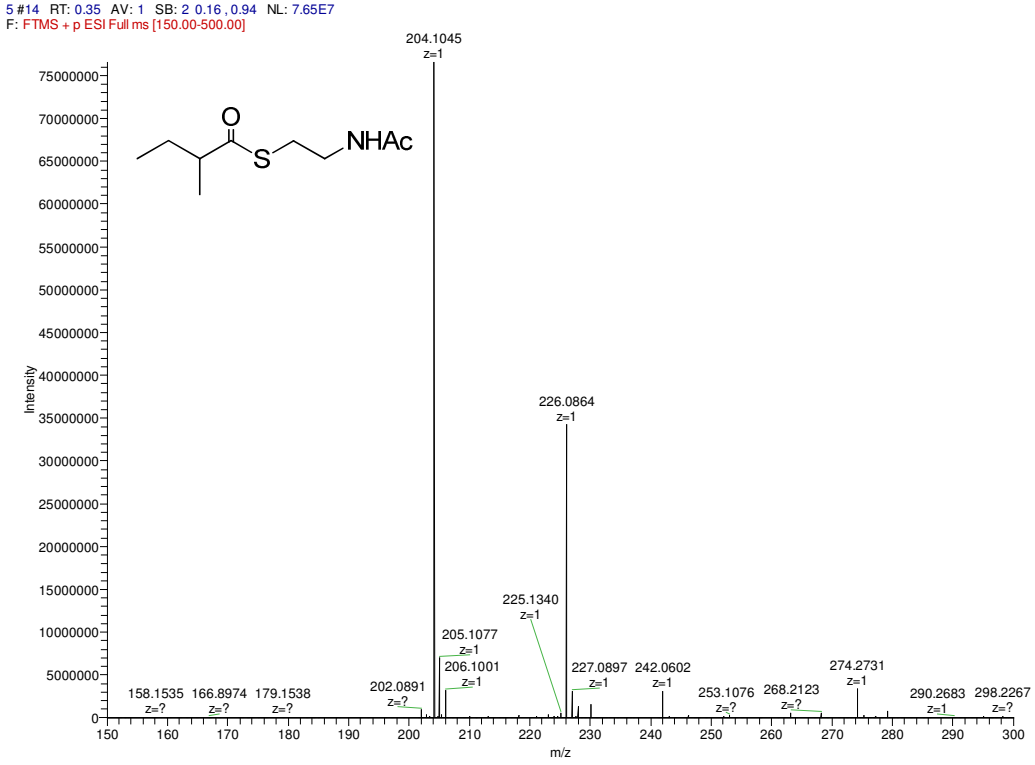

Figure S24. The HRESI mass spectrum of **IV**.

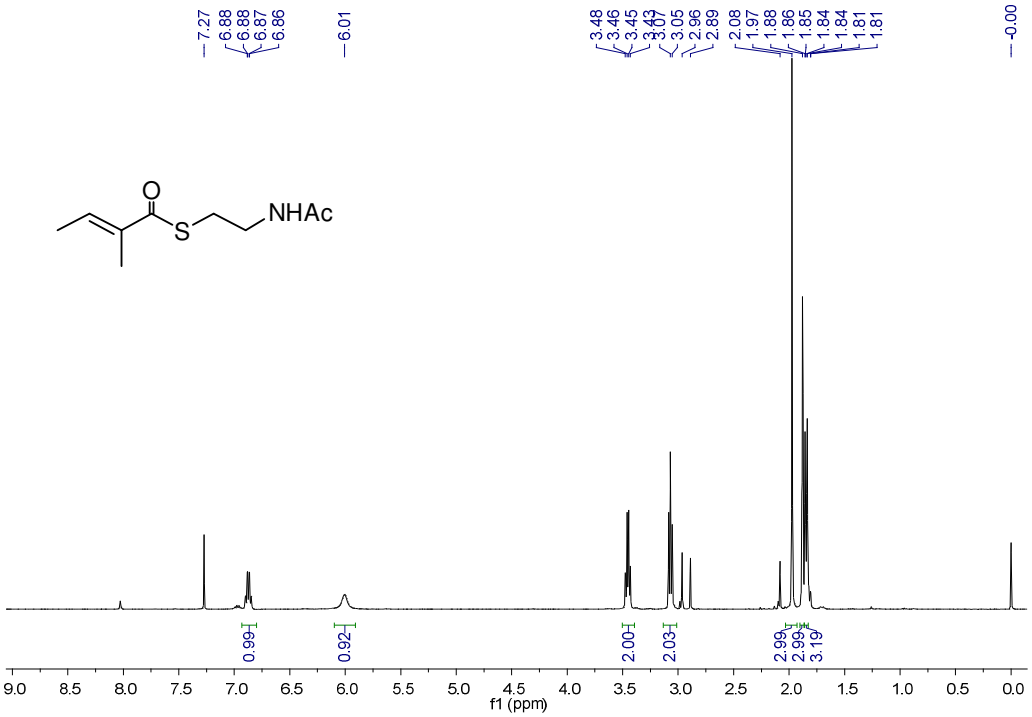

Figure S25. The ^{1}H-NMR (400 MHz, $CDCl_3$, r.t.) spectrum of **V**.

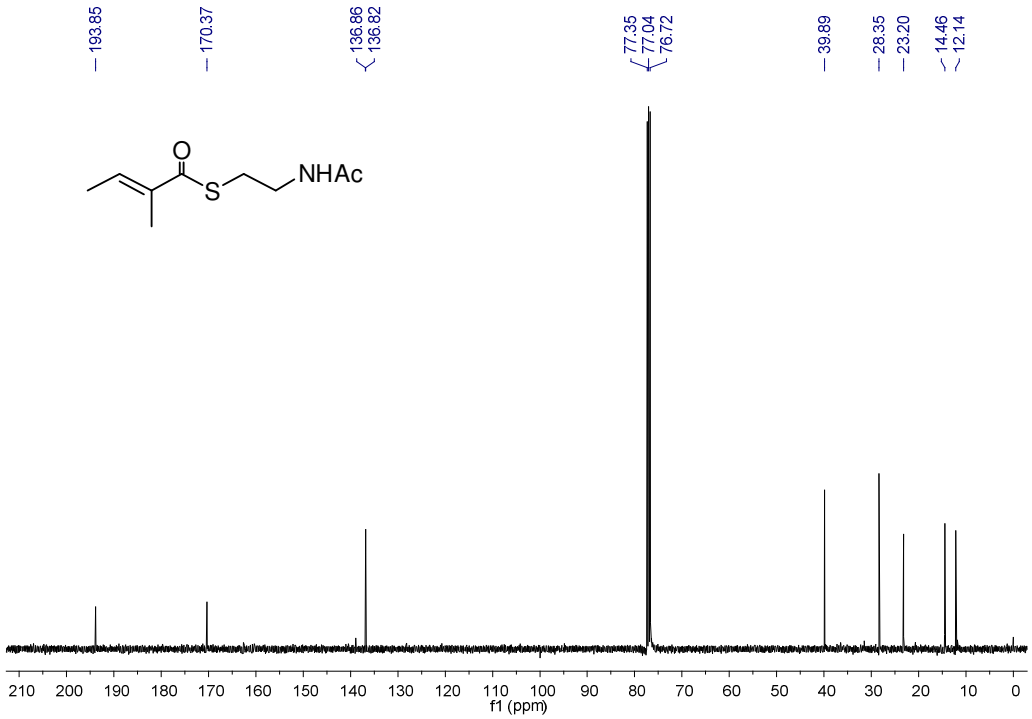

Figure S26. The ^{13}C-NMR (100 MHz, $CDCl_3$, r.t.) spectrum of **V**.

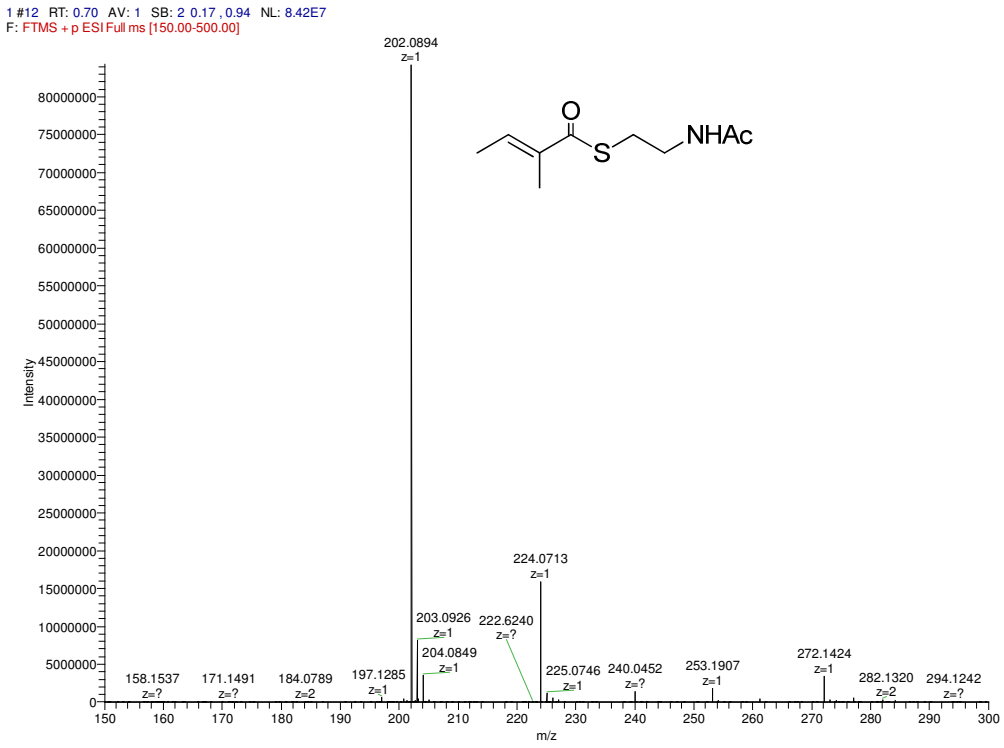

Figure S27. The HRESI mass spectrum of **V**.

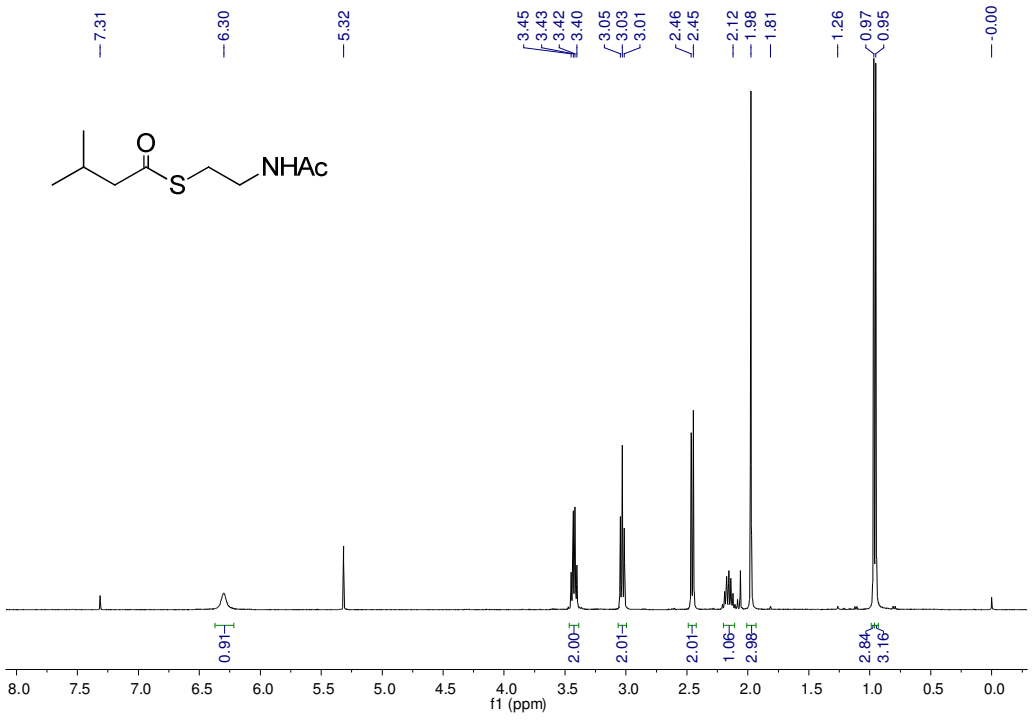

Figure S28. The ^{1}H-NMR (400 MHz, $CDCl_3$, r.t.) spectrum of **VI**.

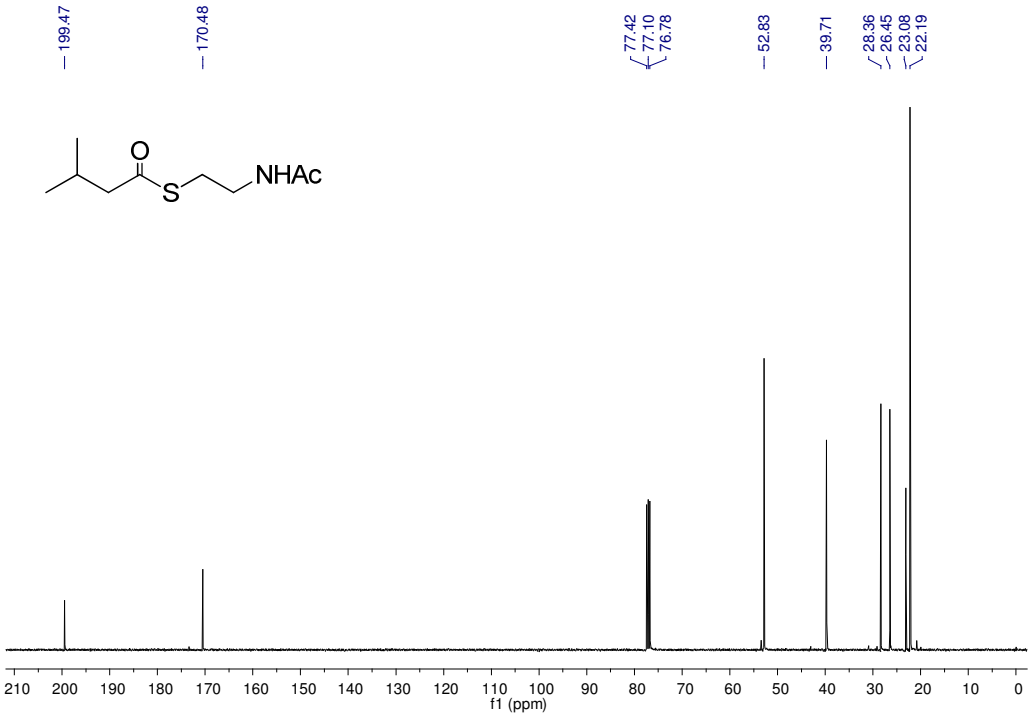

Figure S29. The ^{13}C-NMR (100 MHz, $CDCl_3$, r.t.) spectrum of **VI**.

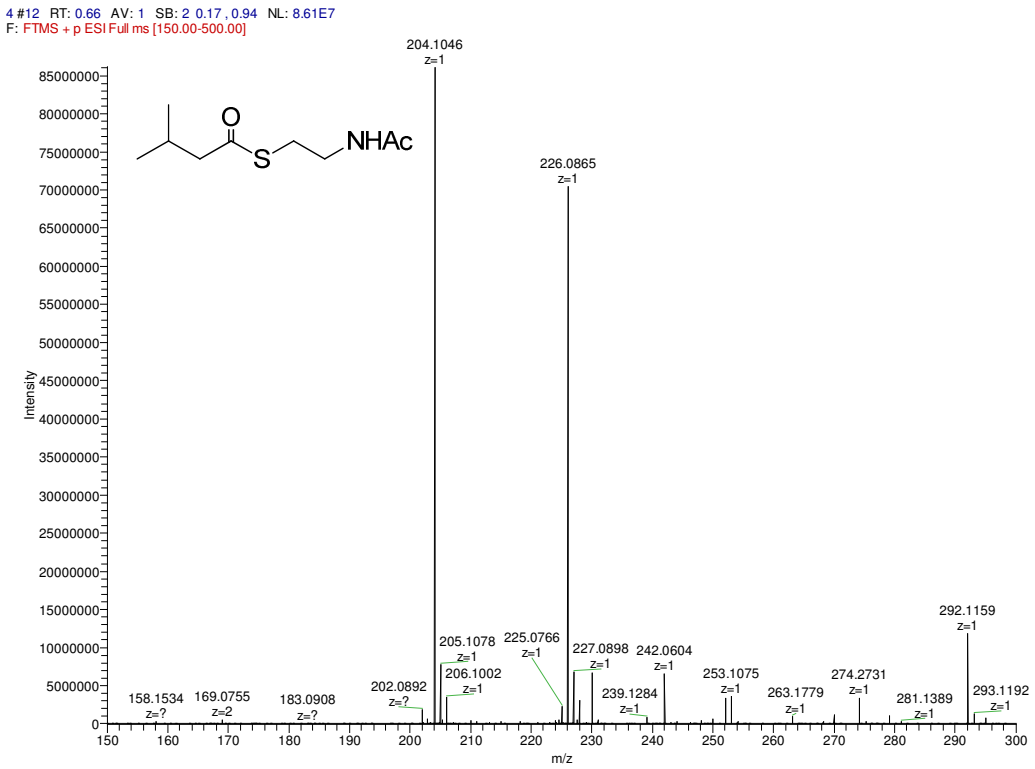

Figure S30. The HRESI mass spectrum of **VI**.

Supplementary References

(1) Paget, M. S., Chamberlin, L., Atrih, A., Foster, S. J., and Buttner, M. J. (1999) Evidence that the extracytoplasmic function sigma factor sigmaE is required for normal cell wall structure in *Streptomyces coelicolor* A3(2), *J. Bacteriol. 181*, 204–211.

(2) DeBarber, A. E., Mdluli, K., Bosman, M., Bekker, L. G., and Barry, C. E., 3rd. (2000) Ethionamide activation and sensitivity in multidrug-resistant *Mycobacterium tuberculosis*, *Proc. Natl. Acad. Sci. U S A 97*, 9677–9682.

(3) Wu, Y., Kang, Q., Shen, Y., Su, W., and Bai, L. (2011) Cloning and functional analysis of the naphthomycin biosynthetic gene cluster in *Streptomyces* sp. CS, *Mol. Biosyst. 7*, 2459–2469.

(4) Smokvina, T., Mazodier, P., Boccard, F., Thompson, C. J., and Guerineau, M. (1990) Construction of a series of pSAM2-based integrative vectors for use in actinomycetes, *Gene 94*, 53–59.